

# Active Cancellation of the Electromagnetic Emissions at the Input of a Periodically Operating Motor Inverter by Injecting Synthesized and Synchronized Signals

M.Sc. Michael Gerten, TU Dortmund University, On-board Systems Lab, Dortmund, Germany  
Dr.-Ing. Andreas Bendicks, TU Dortmund University, On-board Systems Lab, Dortmund, Germany  
Prof. Dr.-Ing. Stephan Frei, TU Dortmund University, On-board Systems Lab, Dortmund, Germany

## Abstract

Power electronic systems can be a significant source of electromagnetic emissions. To meet requirements regarding the electromagnetic compatibility, passive filters are conventionally applied which tend to be bulky and heavy. Active filters are a promising alternative. In this contribution, a special variant of active filtering based on synthesized and synchronized signals is applied to a motor inverter. After a brief explanation of the method, the challenges in conjunction with a motor inverter are discussed. Demonstrator results are shown, and optimizations of this setup are presented.

## 1 Introduction

The on-going electrification of vehicles requires an increasing number of power electronic converters for energy conversion and distribution. Due to their switching behavior, these systems can be a significant source of electromagnetic interferences (EMI) which might, e.g., deteriorate the performance of radio frequency communication. To comply with electromagnetic compatibility (EMC) standards, passive filter components are commonly used to reduce the conducted EMI of power electronic systems. As these tend to be bulky, heavy, and expensive, they conflict the objectives of lowering power consumption and increasing the range of vehicles. Active filtering methods can provide a solution to this problem. After a short overview of conventional active EMI filters, the special variant using synthesized and synchronized signals is described. This method has already been applied successfully to reduce the EMI of DC-to-DC converters and is now used on the DC input of a periodically operating motor inverter. The topology and the expected EMI of this use case are presented, and the approach of calculating the cancellation signal using an FFT is outlined. Afterwards, a demonstrator setup and measurement results are presented. The contribution closes with a summary and an outlook.

## 2 Active EMI Reduction

This chapter describes two general methods for active EMI reduction. The first one, i.e. active EMI filters, have already been discussed frequently. The second method is a rather new approach which employs synthesized and synchronized signals.

### 2.1 Active EMI Filters

Active EMI filters (AEF) in general use analog circuitry in feedforward or feedback topologies to measure the electromagnetic disturbances of the power electronic system, create a suitable cancellation signal and inject it

back into the system [1, 2]. Ideally, the cancellation signal causes a destructive interference with the EMI resulting in an undisturbed system. However, due to limitations of the analog hardware, i.e. finite bandwidths [1, 2] and unavoidable delay times [3], a systematic error remains, and the performance declines for higher frequencies [4].

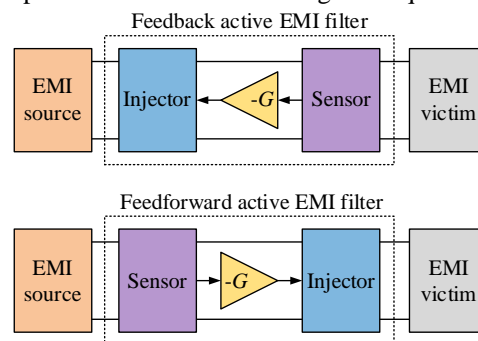
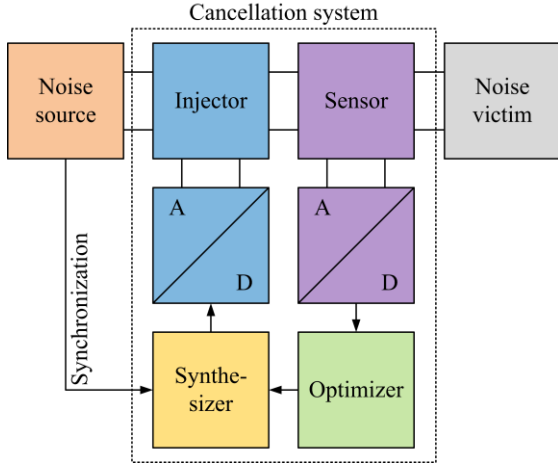


Figure 1: General structures of active EMI filters

### 2.2 EMI Reduction Using Synthesized and Synchronized Signals

To overcome the systematic limitations of AEFs, a new method has been presented in, e.g., [4] and [5], which utilizes synthesized and synchronized cancellation signals ( $S^3$ -AEF). The general structure is depicted in Figure 2. For (quasi-)periodic EMI the cancellation signal can be constructed out of sine waves which each eliminate the disturbing harmonic with the respective frequency. By modifying the amplitude and phase of these sine waves, systematic delay times and frequency responses can be compensated. The correct parameters can be determined by using an optimization algorithm or a system identification approach. The latter is pursued in this work. To ensure the destructive interference between the EMI and the cancellation signal, the  $S^3$ -AEF needs to be exactly synchronized with the power electronic system, e.g., by using the control signals of the transistors as reference. To couple the systems, a suitable sensor and injector circuit are needed for measuring the residual EMI and injecting the cancellation signal, respectively. Signal synthesis and

optimization can conveniently be done on digital hardware. Analog-to-digital and digital-to-analog converters are required as interfaces between the analog and digital domains.



**Figure 2:** Active EMI reduction using synthesized and synchronized signals

### 3 Motor Inverter

This chapter introduces the motor inverter which is investigated in this contribution. First, the topology and the control scheme are described, afterwards the resulting EMI is analyzed.

#### 3.1 Topology

The topology of the investigated motor inverter consists of a half-bridge for each of the three phases of the motor, as depicted in Figure 5. Since the used transistors of the half-bridges can conduct currents in backward direction, no additional antiparallel diodes are needed. A capacitor stabilizes the DC input voltage.

#### 3.2 Control scheme

The three-phase system, which is required to drive the motor, is created by the switching half-bridges. This is usually done by a closed-loop control algorithm. However, this approach will most likely result in switching patterns that differ from each other in each fundamental period. This leads to non-periodic EMI which is disadvantageous for analytical evaluations and makes the calculation of cancellation signals more complex. Therefore, this paper uses an open-loop control for first analysis and proof of concept. The PWM switching patterns, as depicted in Fig. 3, are the result of comparing the reference signal, in this case a sine wave with the fundamental angular frequency  $\omega_0 = 2\pi f_0$ , with a sawtooth signal with a much higher angular frequency  $\omega_c = 2\pi f_c$ , called carrier or switching frequency. Figure 3 (lower graph) shows the resulting voltage at an exemplary switching node. The reference signals of the three half-bridges each have a phase shift of  $120^\circ$ .

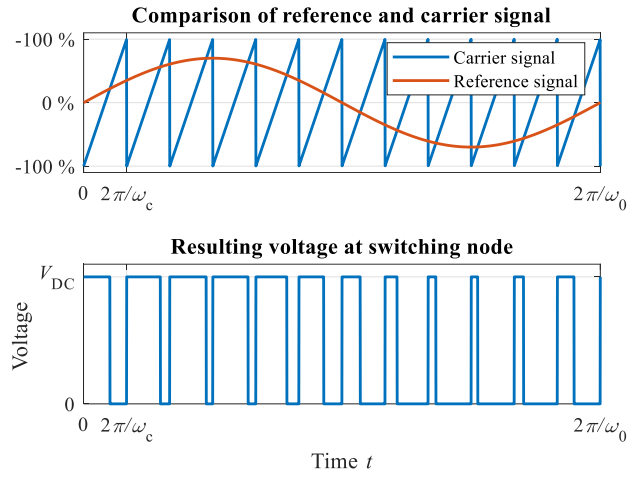


**Figure 3:** PWM signal generation of an exemplary switching node

### 3.3 Resulting EMI

In this section, the EMI of a motor inverter is discussed. As already explained, the three phases of the motor are supplied with PWM voltages. Depending on the switching states of the transistors, the switching events result in a superimposed current  $I_{EMI}$ , which acts as the interference source for the power supply of the inverter (see Figure 5). This EMI current is being smoothed by the input capacitance, yet significant conducted emissions usually remain, which can be measured at the artificial network (AN). The frequency spectrum of the PWM voltage is described analytically in [6]. A generalized version of this spectrum is depicted in Figure 4. It basically consists of three different types of harmonics: baseband harmonics, i.e. harmonics of the fundamental frequency  $\omega_0$ , carrier harmonics of the carrier frequency  $\omega_c$ , and sideband harmonics which are clustered around the carrier harmonics with a spacing of  $\omega_0$ . As shown in [7], this structure also applies for the spectrum of the superimposed current  $I_{EMI}$ .

The baseband harmonics are located at very low frequencies, typically up to a few hundred hertz. As there are usually no EMC limits in this frequency range, these harmonics shall not be suppressed within this contribution. The carrier and sideband harmonics however are of much higher frequencies and can cause radio frequency interference. Therefore, these harmonics shall be actively suppressed in this contribution.

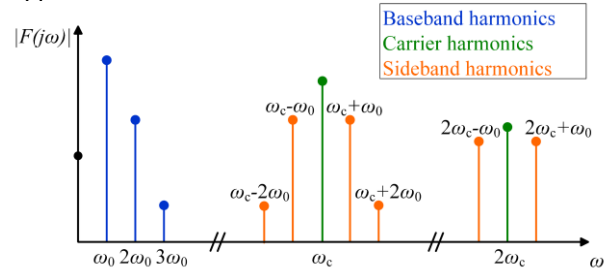


**Figure 4:** Exemplary depiction of the different harmonics of a PWM signal for the control of motor inverters

## 4 Method for EMI Cancellation

This chapter presents the applied method for active EMI reduction using synthesized and synchronized cancellation signals. This method is fundamentally based on an FFT and has already been successfully applied to, e.g., multiple ports of a DC-to-DC converter in [8].

With the FFT approach, the cancellation signal is synthesized in frequency domain. First the EMI is measured in time domain, transformed into frequency domain, processed, and finally transformed back into time domain. Due to unavoidable processing time this method is only applicable if the disturbances are periodic for a sufficient time.

The superposition  $V_{\text{total}}^{\text{sense}}(f)$  of the EMI  $V_{\text{EMI}}^{\text{sense}}(f)$  and the cancellation signal  $V_{\text{anti}}(f)$  at the sensor can mathematically be described as follows (also refer to Figure 5):

$$V_{\text{total}}^{\text{sense}}(f) = V_{\text{EMI}}^{\text{sense}}(f) + H_{\text{anti}}^{\text{sense}}(f) \cdot V_{\text{anti}}(f) \quad (1)$$

$H_{\text{anti}}^{\text{sense}}(f)$  represents the transfer function of the cancellation signal from its injection source to the sensing circuit. For a successful EMI cancellation this superposition  $V_{\text{total}}^{\text{sense}}(f)$  should equal 0 V. Therefore, the necessary cancellation signal can be calculated by (2):

$$V_{\text{anti}}(f) = -\frac{V_{\text{EMI}}^{\text{sense}}(f)}{H_{\text{anti}}^{\text{sense}}(f)} \quad (2)$$

The disturbances  $V_{\text{EMI}}^{\text{sense}}(f)$  at the sensor can simply be measured if the inverter is turned on and the cancellation system is deactivated. The transfer function  $H_{\text{anti}}^{\text{sense}}(f)$  can be determined by, e.g., injecting test signals and evaluating the resulting system response.

The method can be applied iteratively to minimize the residual EMI. These residual disturbances are measured and a new cancellation signal is calculated according to (2). This new signal can then be added to the existing cancellation signal.

## 5 Demonstrator

The schematic of the realized demonstrator is depicted in Figure 5. An FPGA evaluation system Red Pitaya STEMLab 125-14 is used for controlling the inverter. In this

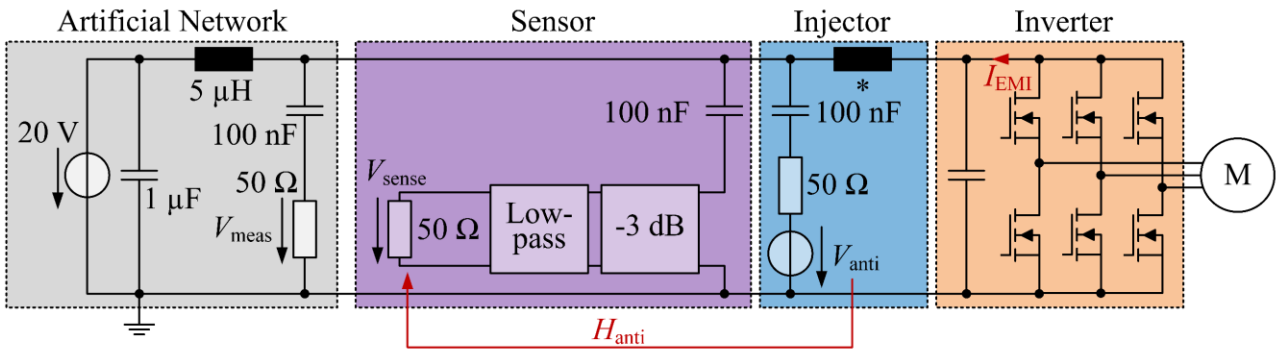
contribution, the system is operated with an input voltage of 20 V and without a mechanical load.

The conducted emissions of the system are measured according to the automotive standard CISPR 25 [9] with an AN and an EMI test receiver (9 kHz bandwidth and at least 50 ms measuring time). The goal is to actively suppress the harmonics in the range of the LW (150 kHz-300 kHz) and MW (530 kHz-1.8 MHz) band. As 50 Hz is used as the base frequency, there is a total of  $(1.8 \text{ MHz} - 150 \text{ kHz})/50 \text{ Hz} + 1 = 33,001$  switching and sideband harmonics to be suppressed. Therefore, the cancellation signal needs to be constructed out of 33,001 sine waves.

The cancellation signal is generated by an arbitrary waveform generator (AWG) of the Tektronix AFG3000 series, which is synchronized to the inverter control. For injection of the cancellation signal a capacitor is used, which is decoupled from the low-impedance inverter through a snap-on MnZn ferrite 742 727 22 from Würth Elektronik [5]. Without this ferrite a large portion of the injected current would flow through the input capacitance of the inverter and not contribute to the intended EMI cancellation at the sensor and AN.

A capacitive sensing circuit is used, which acts as a high pass filter. The measurement is performed by an HDO6104A oscilloscope from Teledyne LeCroy which is also synchronized to the inverter. For a precise measurement of the relevant frequency range, the signal is limited by a low-pass filter with a 2.5 MHz cutoff frequency. An additional 3 dB attenuator is added to avoid resonances between the low-pass filter and the overall system. The input impedance of the oscilloscope is set to 50  $\Omega$ . Its vertical resolution is adapted every iteration to measure as precisely as possible.

The measured voltage values are transferred to a PC running MATLAB to synthesize the necessary cancellation signal according to section 4. The determined signal is then transferred to the AWG which injects it into the system. The realized inverter is shown in Figure 6. The half-bridges are evaluation boards EPC9033 from EPC and use GaN-based transistors. They are operated with a switching frequency  $f_c$  of 100 kHz. The FPGA system for inverter control is built into the inverter box. The synchronization signal for the oscilloscope and the AWG is passed by a BNC feedthrough. The cancellation signal coming from



\*MnZn 742 727 22

Figure 5: Schematic of the demonstrator setup

the AWG and the sensor signal going to the oscilloscope are also connected via BNC feedthroughs.

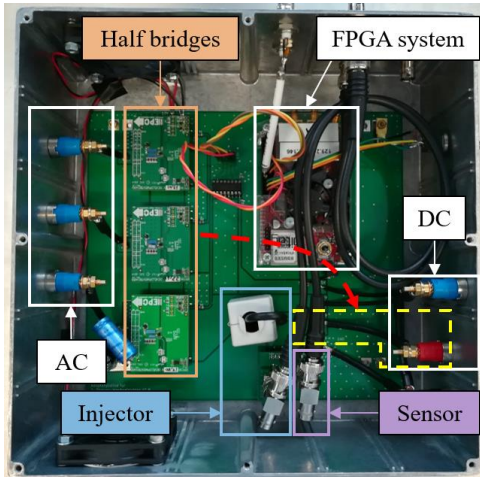


**Figure 6:** Realized inverter with sensor and injector. Yellow and red: Potential coupling path between sensor and DC input (as discussed in Section 6.2)

## 6 Measurement Results

In the following chapter, measurement results of the demonstrator setup are presented. Arising difficulties are discussed and possible optimizations are investigated.

### 6.1 First result

The initial result of applying the proposed EMI reduction method to the demonstrator is shown in Figure 7. The active cancellation system significantly reduces the switching and sideband harmonics in the examined frequency range from 150 kHz to 1.8 MHz. The switching harmonic at 200 kHz is suppressed by about 33 dB, the switching harmonic at 1.8 MHz is reduced by 10 dB. Since preliminary investigations with a similar disturbing signal showed much higher EMI reductions, it is assumed that the system’s behavior is restricting the achievable reduction. Therefore, different optimizations are evaluated in the following paragraphs.

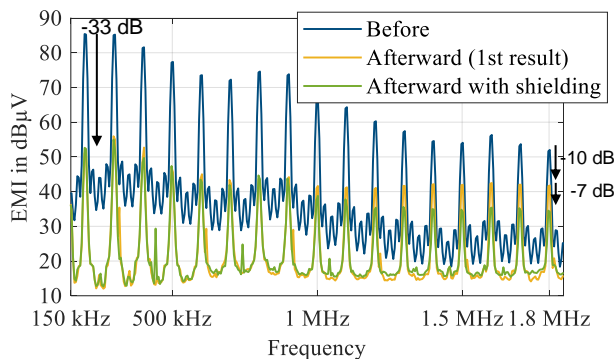


**Figure 7:** Measured EMI at the artificial network: (1) active cancellation system installed but deactivated, (2) with active cancellation, (3) with active cancellation and shielding of input cables

### 6.2 Optimization: Shielding of parasitic coupling

The cancellation system reduces the EMI which is measured at the location of the sensor. It could be found that the EMI reduction directly at the sensor is higher than the one at the AN. Therefore, it can be assumed that some disturbances couple into the path between sensor and DC input of the inverter box, possibly caused by the steep voltage slopes at the switching nodes of the half bridges (refer to red and yellow marking in Figure 6). Thus, although the injected signal cancels out the EMI directly at the sensor, additional EMI is coupling over the sensor can then be measured at the AN. To reduce this potential parasitic coupling, the path between DC input and sensor is shielded by a grounded copper tape. Additional copper tape is used to improve the ground connection of sensor and injector, resulting in the setup shown in Figure 8. These measures helped to optimize the EMI reduction according to Figure 7. Compared to the unoptimized setup, the active suppression is now up to 7 dB greater, primarily in the higher frequency range. This strengthens the assumption of parasitic coupling, as the field coupling is expected to have a greater effect for higher frequencies. Despite this improvement, the resulting EMI reduction is still worse than in preliminary investigations with a motor emulation consisting of resistors and inductors. So, it is assumed that the rotating machine alters the EMI in such a way that is not respected in the synthesis method for the cancellation signal. This is elaborated in the next section.

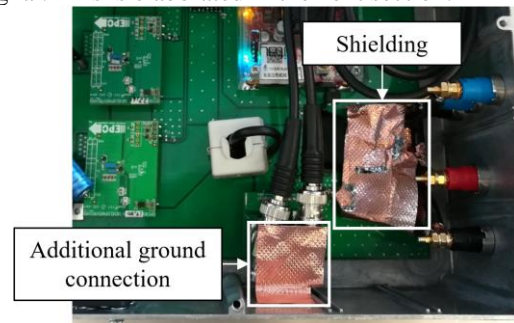


**Figure 8:** Shielding of a potential coupling path and additional grounding of sensor and injector

### 6.3 Optimization: Consideration of the mechanical rotational frequency

Up to this point, the EMI was expected to repeat itself with the fundamental frequency of the three-phase system (50 Hz). The motor, however, has 4 pole pairs and therefore rotates with a reduced frequency of 12.5 Hz. To investigate if this influences the resulting electromagnetic disturbances, they were recorded at the AN over a length of eight periods (8·20 ms = 160 ms). Part of this signal’s spectrum (found by an FFT) is shown in Figure 9. The highest harmonics have a spacing of 50 Hz to each other, These were already considered in the previous calculations. Additionally, there are also harmonics with a spacing of 12.5 Hz that have significant amplitude levels. These seem to result from the mechanical rotational frequency of the motor, which supports the hypothesis that

the EMI is actually repeating itself with the mechanical instead of the electrical frequency. Since eight signal periods were recorded, there are also harmonics with a spacing of 6.25 Hz (1/160 ms), but their low amplitude levels can be expected to be measurement noise.

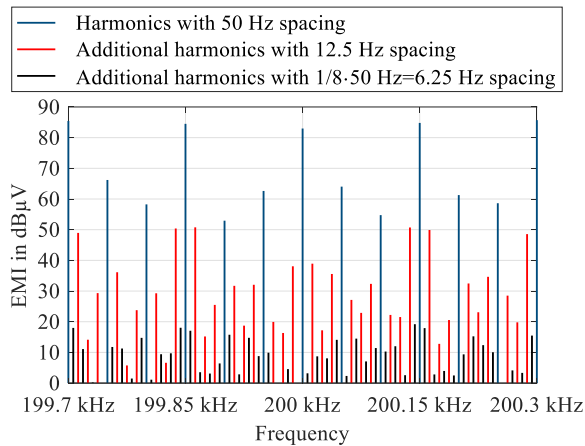


**Figure 9:** Measured harmonics at the artificial network

Therefore, a cancellation signal is created that also suppresses the additional harmonics with 12.5 Hz spacing. The signal length is now four times as long as before. Since the AWG's memory depth is limited, the sampling time must be increased. Thus, according to Nyquist's theorem, only the switching harmonics at 200, 300, 400 and 500 kHz and their sideband harmonics can be suppressed with the used setup. The results are depicted in Figure 10 and show that the performance could be significantly improved, leading to a reduction of at least 40 dB for the four considered harmonics.

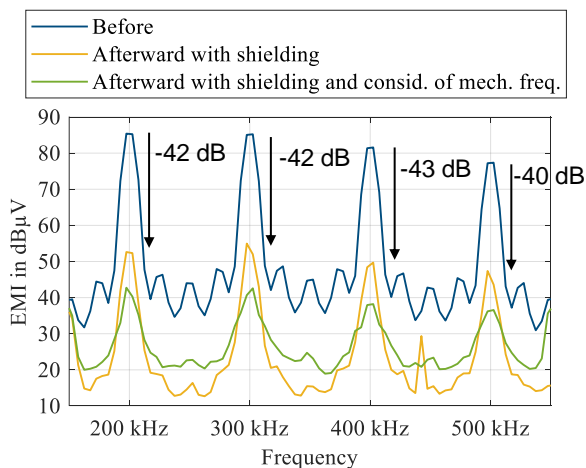


**Figure 10:** EMI reduction after consideration of the mechanical rotational frequency

## 7 Conclusion

In this contribution the method of active EMI reduction using synthesized and synchronized cancellation signals was applied to a motor inverter. After optimizations, this led to active EMI suppressions of about 40 dB in the frequency range of 200 kHz to 500 kHz. Harmonics up to 1.8 dB could be reduced by more than 17 dB.

It was elaborated that parasitic couplings inside of the system can degrade the effectiveness of the method. Additionally, it was shown that the EMI repeats with the fundamental mechanical frequency instead of the electrical frequency, which increased the number of harmonics by the factor of the number of pole pairs (in this case four). Further investigations should be performed with an optimized mechanical design of the inverter and show the effectiveness of the method under higher power.

## 8 Acknowledgment

The results of this publication go partly back to the project RobKom ("Robuste Kommunikation in autonomen Elektrofahrzeugen", grant number 16EMO0380) supported by the German Federal Ministry of Education and Research (BMBF). The responsibility for this publication is held by the authors only.

## 9 Literature

- [1] Y.-C. Son, S.-K. Sul: "Generalization of active filters for EMI reduction and harmonics compensation". In IEEE Transactions on Industry Applications, vol. 42, no. 2, pp. 545-551, Mar./Apr. 2006
- [2] N. K. Poon, J. Liu, C. K. Tse, M. H. Pong: "Techniques for input ripple current cancellation: classification and implementation [in smps]". In IEEE Transactions on Power Electronics, vol. 15, no. 6, pp. 1144-1152, 2000
- [3] B. Arndt, P. Olbrich, H. Reindl, C. Waldera: „Breitbandiger aktiver Hybrid-Filter für Kfz-Anwendungen“. In EMV Düsseldorf, Düsseldorf, Germany, 20.-22.02.2018, pp. 432-438
- [4] A. Bendicks, "Active Cancellation of Electromagnetic Emissions of Power Electronic Systems by Injecting Synthesized and Synchronized Signals," Ph.D. dissertation, On-board Systems Lab, TU Dortmund University, Dortmund, Germany, 2020. [Online]. Available: <https://eldorado.tu-dortmund.de/handle/2003/39212?locale=en>.
- [5] A. Bendicks, S. Frei: "Broadband noise suppression of stationary clocked dc/dc converters by injecting synthesized and synchronized cancellation signals". In IEEE Transactions on Power Electronics, vol. 34, no. 11, pp. 10665-10674, 2019
- [6] D. G. Holmes, T. A. Lipo: "Pulse Width Modulation for Power Converters: Principles and Practice". Ed. 1, Wiley-IEEE Press, 2003
- [7] B. P. McGrath, D. G. Holmes: "A general analytical method for calculating inverter dc-link current harmonics", In IEEE Transactions on Industry Applications, vol. 45, no. 5, pp. 1851-1859, Sept./Oct. 2009
- [8] A. Bendicks, M. Rübartsch, S. Frei: „Simultaneous EMI Suppression of the Input and Output Terminals of a DC/DC Converter by Injecting Multiple Synthesized Cancellation Signals“. In EMC Europe, Barcelona, Spain, 02.-06.09.2019, pp. 842-847

- [9] CISPR 25: “Vehicles, boats and internal combustion engines – Radio disturbance characteristics – Limits and methods of measurement for the protection of on-board receivers“. 4th ed., Feb. 2015